Semiclassical investigation of revival phenomena in one dimensional system

Zhe-xian Wang [1] Eric J. Heller [2]

1 Hefei National Laboratory for Physical Sciences at Microscale and Department of Physics, University of Science and Technology of China, Hefei, Anhui 230026, P. R. China

2 Department of Physics and Department of Chemistry and Chemical Biology, Harvard University, Cambridge, Massachusetts 02138, USA

Abstract

In a quantum revival, a localized wavepacket re-forms or "revives" into a compact reincarnation of itself long after it has spread in an unruly fashion over a region restricted only by the potential energy. This is a purely quantum phenomenon, which has no classical analog. Quantum revival, and Anderson localization, are members of a small class of subtle interference effects resulting in a quantum distribution radically different from the classical after long time evolution under classically nonlinear evolution. However it is not clear that semiclassical methods, which start with the classical density and add interference effects, are in fact capable of capturing the revival phenomenon. Here we investigate two different one dimensional systems, the infinite square well and Morse potential. In both cases, after a long time the underlying classical manifolds are spread rather uniformly over phase space and are correspondingly spread in coordinate space, yet the semiclassical amplitudes are able to destructively interfere over most of coordinate space and constructively interfere in a small region, correctly reproducing a quantum revival. Further implications of this ability are discussed.

Key words: Quantum revival, Semiclassical, Infinite square well, Morse potential
PACS: 03.65.Sq, 42.50.Md

1 Introduction

The phenomenon of "quantum revival" attracted much attention after it was first studied in quantum electrodynamics [1,2]. The evolution of a quantum wave packet in a general smooth potential has at least three regimes. First, an initially localized packet will evolve following classical mechanics for a time,

in the sense that the mean position and momentum of the wave packet follow classical laws. More than that, the spreading of the wave packet follows an analogous classical distribution with appropriate initial position and momentum densities. This is the Ehrenfest regime.

After further evolution, after the wave packet has become delocalized, interference effects may become important, causing the classical distribution and the quantum wave packet to have quite different details. Semiclassical methods however are expected to be working well. They are based solely on classical information, but incorporate interference effects by assigning an amplitude and phase for the multiple classical paths which connect to each final position:

$$\psi(x,t) = \sum_n \sqrt{P_n(x,t)}\; e^{i\,\phi_n(x,t)/\hbar} \tag{1}$$

where $P_n(x)$ is the classical probability density for the n^{th} way of reaching x give the initial classical manifold and $\phi_n(x,t)$ is the classical action along the n^{th} path reaching x. The Born interpretation, namely that $\psi(x,t)$ is a probability amplitude, dictates that the wavefunction should go as the square root of the classical probabilities in the correspondence limit.

After a very long period of time, many classical periods in the case of an oscillator, the quantum wave packet will reverse its seemingly unorganized delocalized oscillation to neatly rebuild into its initial form. This is the known quantum revival, the third regime. Quantum revival has been widely investigated in atomic [3,4,5] and molecular [6,7,8] wave packet evolution and other quantum mechanics systems [9,10,11,12,13]. An excellent review on wave packet revivals is given by Robinett [14]. Precursors to the full revival also exist, in which other organized probability distributions develop [14]. The question addressed in this paper is: is the third, revival regime also semiclassical? May we think of revival in semiclassical terms after all, i.e. classical mechanics with phase interference included? It is a tall order for semiclassical sums to self cancel almost everywhere the classical density is large, with the exception of one region where the revival is occurring.

Time dependent semiclassical methods are exact in the limit of short time, being equivalent to the short time limit of the quantum propagator. Increasing time can only degrade the results. At long times, the number of terms in the sum, Eq. 1 can become very large, and in fact the number of terms grows exponentially in chaotic systems. This in itself does not spell the breakdown of semiclassics. In earlier work on chaotic systems, Tomsovic et. al. [15] showed that semiclassical amplitudes were doing well when more than 6000 terms were needed in the sum. Other work justified the unexpected accuracy of the semiclassical results [16]. Later, Kaplan [17] gave an ingenious analysis of the breakdown with time in the case of chaotic systems, which built on earlier the analyses [16] indicating that classical chaos rather surprisingly *aided*

accurate semiclassical propagation. The implication was that even Anderson localization was describable semiclassically, albeit with an astronomical number of terms in the sum, Eq. 1. Quantum revival in a potential well does not involve chaotic spreading in phase space, and thus it could be more difficult to describe correctly semiclassically, give the arguments in the above references about the benefits of chaotic flow.

The revival phenomenon has no purely classical analog. At best it is a semiclassical effect, describable in the terms of Eq. 1. The classical analog of a localized wave packet will be a continuous density of trajectories in phase space, well localized but consistent with the uncertainly principle. In an anharmonic oscillator, these trajectories occupy a distribution of energies and hence frequencies. The distribution spreads and begins to wind itself up on a spiral (see below), with many branches at a typical position. A smooth distribution of trajectories with a range of velocities and positions, after spreading evenly into the available space, will never converge again on one locale. This seems quite contradictory to the quantum result. Semiclassical theory can bridge the gap between classical and quantum field, and provide a simple and intuitive way to understand the subtle issue of quantum revival.

In this paper we study the quantum revival in both infinite square well and Morse potential system. These two cases are quite different in detail. The square well is locally linear, interrupted by discontinuities which are due to reflections at the walls. The Morse potential is more typical, arriving at its nonlinear evolution smoothly. Semiclassical results are analytic whenever the dynamics is "linear". Examples are the free particle, the linear ramp potential, and the harmonic oscillator. In each case, current positions and momenta are linear functions of initial positions and momenta. The square well is not in fact a linear system, because of reflections at the walls. However, locally, the classical manifolds evolve linearly, suffering truncation due to the reflections (see Figure 1). Interestingly the square well is a case with (globally) nonlinear time evolution clearly showing revivals, yet because of the locally linear nature of the classical dynamics the semiclassical formula turns out to be exact. When the semiclassical method is approximate, the delicate cancellation of amplitudes over wide areas is in question, and we show here by example that it is still accurate enough to give the revivals.

2 Theory

Time-dependent semiclassical methods face difficulties when applied to long revival time calculations. By their very nature, revivals cannot happen until the classical manifolds have folded over on themselves many times, which means the dynamics is in the deeply nonlinear regime. Although nothing keeps

semiclassical methods from working under these conditions in principle, and practice the error can only grow with time. If one is looking at a subtle phenomenon, such as near exact cancellation of semiclassical amplitudes over a wide area, the small errors could be a problem.

A convenient way to implement the semiclassical method is via cellular dynamics [20], which has been proven to be accurate and efficient for longtime implementation of semiclassical calculations. The basic idea is to linearize the classical dynamics in zones small enough to make the linearization classically correct. The zones are typically much smaller than Planck's constant in area. In the following, a brief summary of cellular dynamics is given. In the next section we discuss the revival in both infinite square well and Morse potential systems. Further speculations are given in the Conclusion.

The starting point of semiclassical method is the Van-Vleck-Gutzwiller (VVG) propagator [21]

$$\begin{aligned} G\left(x,x_0;t\right) &= \left(\frac{1}{2\pi \mathrm{i}\hbar}\right)^{1/2} \sum_j \left|\frac{\partial^2 S_j(x,x_0)}{\partial x \partial x_0}\right|^{1/2} \exp\left[\frac{\mathrm{i}S_j(x,x_0)}{\hbar} - \frac{\mathrm{i}\nu_j\pi}{2}\right] \\ &= \left(\frac{1}{2\pi \mathrm{i}\hbar}\right)^{1/2} \sum_j \left|\frac{\partial x}{\partial p_0}\right|^{-1/2} \exp\left[\frac{\mathrm{i}S_j(x,x_0)}{\hbar} - \frac{\mathrm{i}\nu_j\pi}{2}\right], \end{aligned} \tag{2}$$

where action $S(x,x_0) = \int_0^t dt' \left[p\left(t'\right)\dot{x}\left(t'\right) - H\left(p\left(t'\right),x\left(t'\right)\right)\right]$ is the integral of the Lagrangian along classical trajectory from x_0 to x, and Maslov index ν counts the number of caustic points along this trajectory. The sum over j runs over all the trajectories connecting x_0 to x, in other words, it counts in contributions from all the stationary phase points. Cellular dynamics begins with a transformation of the propagator by applying the speciality of δ function:

$$\sum \frac{1}{\left(\partial x_t/\partial p_0\right)|_{x=x_t}} = \int dp_0 \delta\left(x - x_t\left(x_0,p_0\right)\right). \tag{3}$$

Here $x_t\left(x_0,p_0\right)$ is the final position originate from initial point (x_0,p_0). The VVG propagator can now be written as

$$G\left(x,x_0;t\right) = \left(\frac{1}{2\pi i\hbar}\right)^{1/2} \int dp_0 \left|\frac{\partial x_t}{\partial p_0}\right|_{x_0}^{1/2} \delta\left(x - x_t\left(x_0,p_0\right)\right) \exp\left[\frac{iS\left(x_0,p_0\right)}{\hbar} - \frac{i\upsilon\pi}{2}\right], \tag{4}$$

with the change of action S as a function of (x_0,p_0). Then we can get the

semiclassical wave function

$$\begin{aligned}\psi(x,t) &= \int dx_0 G(x,x_0;t)\,\psi(x_0,0) \\ &= \left(\frac{1}{2\pi i\hbar}\right)^{1/2} \int dx_0 \int dp_0 \left|\frac{\partial x_t}{\partial p_0}\right|^{1/2} \delta(x-x_t)\, e^{iS/\hbar - i\nu\pi/2}\psi(x_0,0).\end{aligned} \tag{5}$$

It would be difficult evaluate the integral directly since it is highly oscillatory. However, cellular dynamics handles this difficulty by using integration techniques similar in spirit to Filinov methods, by dividing the region into small cells, inserting the identities $1 \approx \eta \sum_n \exp[-\alpha (x-x_n)^2]$ within both x and p space. Then we have

$$\begin{aligned}\psi(x,t) = \eta\eta' \sum_n \sum_m \int dx_0 \int dp_0 \left|\frac{\partial x_t}{\partial p_0}\right|^{1/2} \delta(x-x_t) e^{iS/\hbar - i\nu\pi/2} \\ \times e^{-\alpha(x_0-x_n)^2 - \beta(p_0-p_m)^2} e^{-\gamma(x_0-x_i)^2 + ik_i(x_0-x_i)^2},\end{aligned} \tag{6}$$

where the initial wave function $\psi(x_0,0) = \exp\left[-\gamma(x_0-x_i)^2 + ik_i(x_0-x_i)^2\right]$ is used. If both α and β are taken to be sufficiently large, and for sufficiently many cells, we can linearize the classical dynamics around the central trajectory for each cell running from the initial phase space point (x_n, p_m), obtaining its contribution to the propagation of initial wave function.

In some ways cellular dynamics resembles Miller's initial value representation (IVR)[22], but there are important differences. The IVR is actually numerically superior, in that if the integral is performed the result is not the "primitive semiclassical" Van Vleck result, but rather a uniformized version which is capable of describing some classically forbidden processes and of smoothing out some semiclassical singularities. In contrast, cellular dynamics is a direct but numerically convenient implementation of the primitive semiclassical Green's function. The goal of the present paper is to test the efficacy of the primitive semiclassical propagator, but implementing an IVR would be an interesting study.

The linearization is implemented by approximating classical action S with second order Taylor expansion and final position $x(x_0,p_0)$ with first order [20], viz.

$$\begin{aligned}S &\approx S_{nmt} + (p_{nmt}m_{22} - p_m)(x_0-x_n) + p_{nmt}m_{21}(p_0-p_m) \\ &\quad + \tfrac{1}{2}m_{12}m_{22}(x_0-x_n)^2 + \tfrac{1}{2}m_{11}m_{21}(p_0-p_m)^2 \\ &\quad + m_{12}m_{21}(x_0-x_n)(p_0-p_m) \\ x_t(x_0,p_0) &\approx x_{nmt} + m_{21}(p_0-p_m) + m_{22}(x_0-x_n) \qquad .\end{aligned} \tag{7}$$

where S_{nmt}, x_{nmt}, p_{nmt} are the classical action, final position and momentum of a trajectory originate from (x_n, p_m) respectively, and

$$M = \begin{pmatrix} m_{11} & m_{12} \\ m_{21} & m_{22} \end{pmatrix} = \begin{pmatrix} \partial p_t/\partial p_0 & \partial p_t/\partial x_0 \\ \partial x_t/\partial p_0 & \partial x_t/\partial x_0 \end{pmatrix} \tag{8}$$

is the Jacobian matrix of the corresponding dynamical transformation [20]. The substitution of equation (7) into (6) will simplify the quadrature into Gaussian integration

$$\psi(x,t) = \eta\eta' \sum_n \sum_m \int dx_0 \left|\frac{\partial x_t}{\partial p_0}\right|^{-1/2} e^{-a(x_0-x_n)^2+b(x_0-x_n)+c}, \tag{9}$$

with the coefficients

$$\begin{aligned} a =& \alpha + \gamma + \beta\left(\frac{m_{22}}{m_{21}}\right)^2 - \frac{i}{\hbar}\left(\frac{1}{2}\frac{m_{11}m_{22}^2}{m_{21}} - \frac{1}{2}m_{12}m_{22}\right), \\ b =& \frac{2\beta m_{22}}{m_{21}^2}(x - x_{nmt}) - 2\gamma(x_n - x_i) + ik_i \\ &+ \frac{i}{\hbar}[\left(m_{12} - \frac{m_{11}m_{22}}{m_{21}}\right)(x - x_{nmt}) - p_m], \\ c =& -\frac{\beta}{m_{21}^2}(x - x_{nmt})^2 - \gamma(x_n - x_i)^2 - \frac{i\nu\pi}{2} + ik_i(x_n - x_i) \\ &+ \frac{i}{\hbar}[S_{nmt} + p_{nmt}(x - x_{nmt}) + \frac{m_{11}}{2m_{21}}(x - x_{nmt})^2]. \end{aligned} \tag{10}$$

The equation (6) can now be analytically evaluated

$$\psi(x,t) = \eta\eta' \sum_n \sum_m \sqrt{\frac{\pi}{am_{21}}} e^{b^2/4a+c}, \tag{11}$$

and it is easy to implement.

3 Results and discussions

In this section we will analyze the quantum revival in the infinite square well and Morse potential in detail. First we look at the infinite square well system, which has been well studied at many levels and from many points of view [11,12,13]. We take the initial Gaussian of the form

$$\psi(x_0, 0) = \sqrt{\gamma/\pi}\exp\left[-\gamma(x_0 - x_i)^2 + ik_i(x_0 - x_i)^2\right] \tag{12}$$

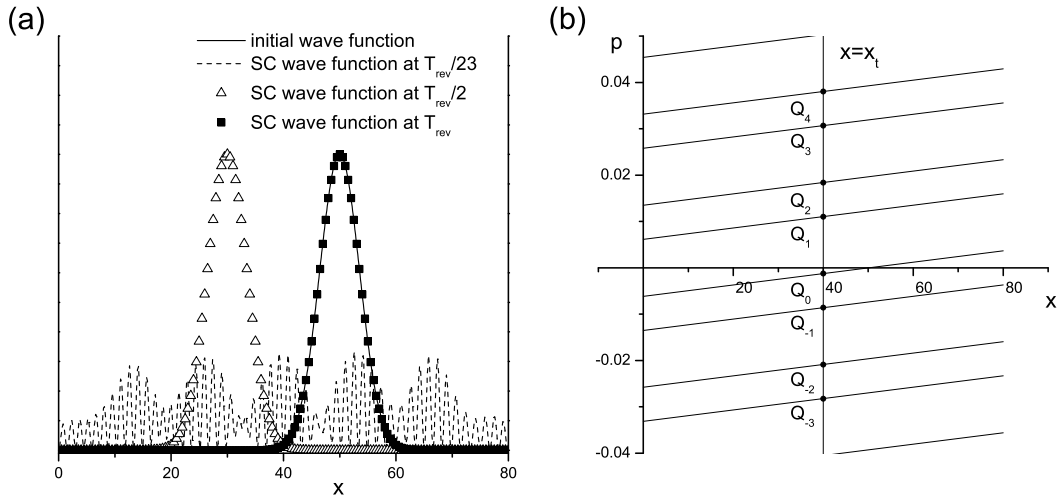

Fig. 1. (a) Semiclassical wave functions evolve in infinite square well at different times. (b) Partial classical manifold of an initial δ function evolves in infinite square well at time T_{rev}.

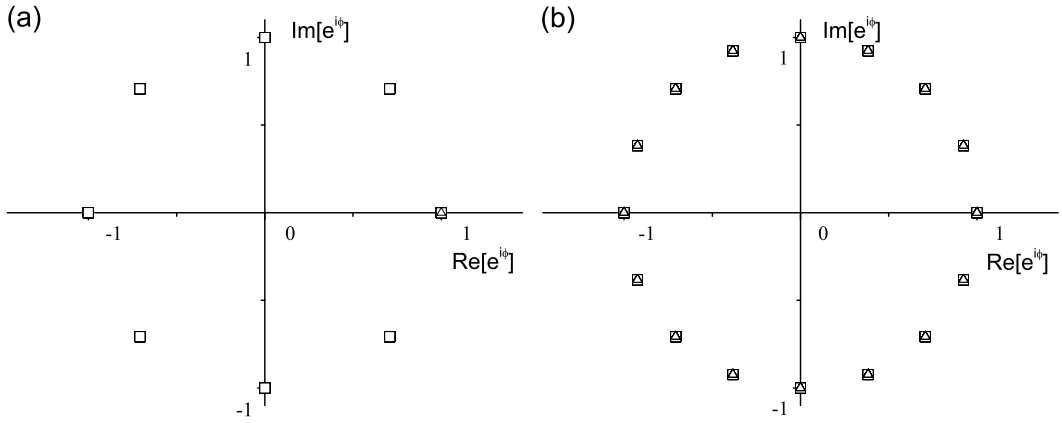

Fig. 2. The distribution of exponential function in complex plane for position (a)$x = 50$; (b)$x = 11$. The square and triangle indicate phase terms come from the first and second exponential function in equation (18) respectively.

and the system Hamiltonian is

$$H = p^2/2m + V(x), V(x) = \begin{cases} 0, 0 < x < L \\ \infty, x \leq 0, x \geq L \end{cases}. \tag{13}$$

In infinite square well system, by expanding the evolving wave function with eigen states, the revival time $T_{rev} = 4mL^2/\hbar\pi$ can be analytically determined [12], and it only depends on electron mass and the width of the well. In all the calculations $m = 1, \hbar = 1$ are used for simplicity. With parameters $\gamma = 0.02, k_i = 2, x_i = 50$ and $L = 80$ we compute the semiclassical wave function at different times using cellular dynamics, we take 100 cells equally spaced in x from 20 to 80 and 1500 cells in p from 0.8 to 3.2. One should pay attention to the Maslov phase here, in hard wall limit it is a multiple of π

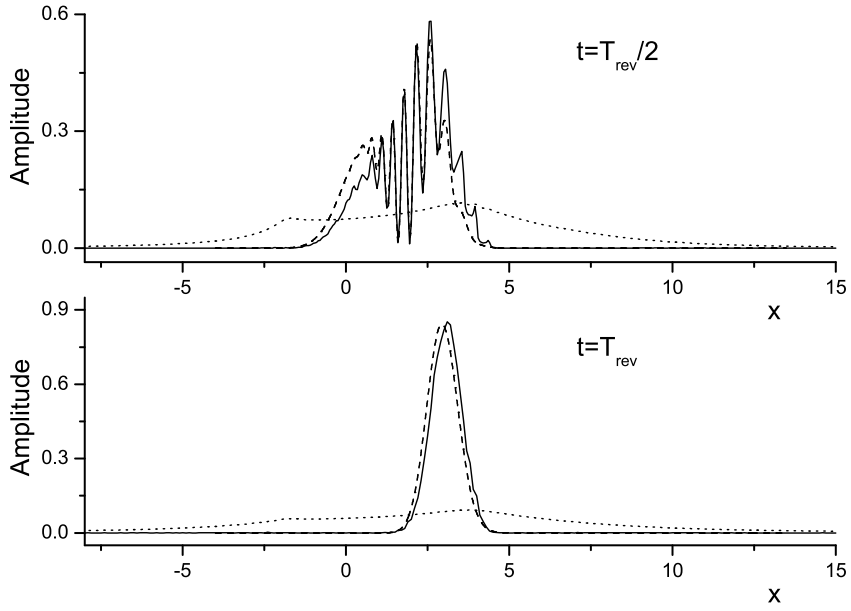

Fig. 3. Wave functions and classical distribution probabilities in Morse potential at time $T_{rev}/2$ and T_{rev}. All the functions plot in this figure are normalized. Solid line: Semiclassical wave functions; Dash line: Exact FFT wave functions calculated by Split-Operator method [23];Dot line: Classical density in coordinate space which evolves from the initial density.

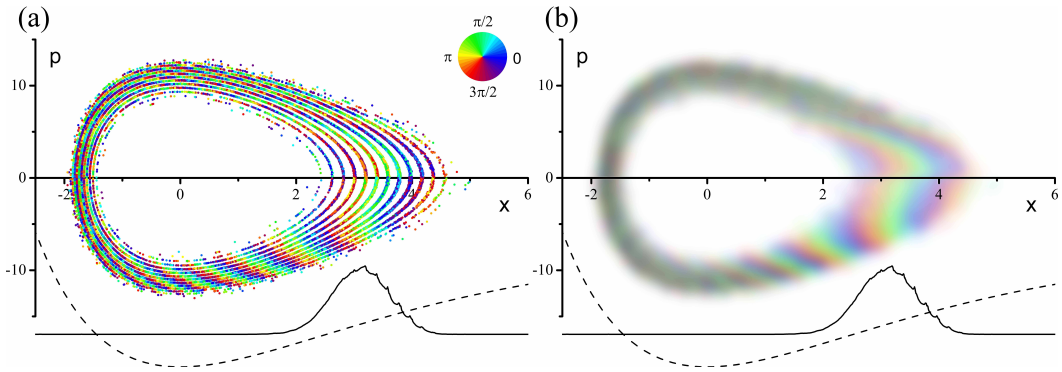

Fig. 4. (a)Phase space diagram for Wigner transformed Gaussian evolves in Morse potential at time T_{rev}. The color indicates different value of phase (include classical action S and Maslov phase) divided by 2π. (b) The blurred version of figure (a). Solid line: semiclassical wave function at time T_{rev}; Dash line: Morse potential.

instead of $\pi/2$. As shown in Fig 1 (a), the wave packet quickly spread over the well after first several classical periods, and at time $t = T_{rev}/2$ the wave function is a mirror image of initial wave function, then after revival time T_{rev} the wave function is perfectly rebuilt into initial wave packet. The reason we suggest for this astonishing relocalize of wave packet is the interference between different contributing classical trajectories. In the following we unfold our discussions.

As the revival in infinite square well is independent of the shape of the wave

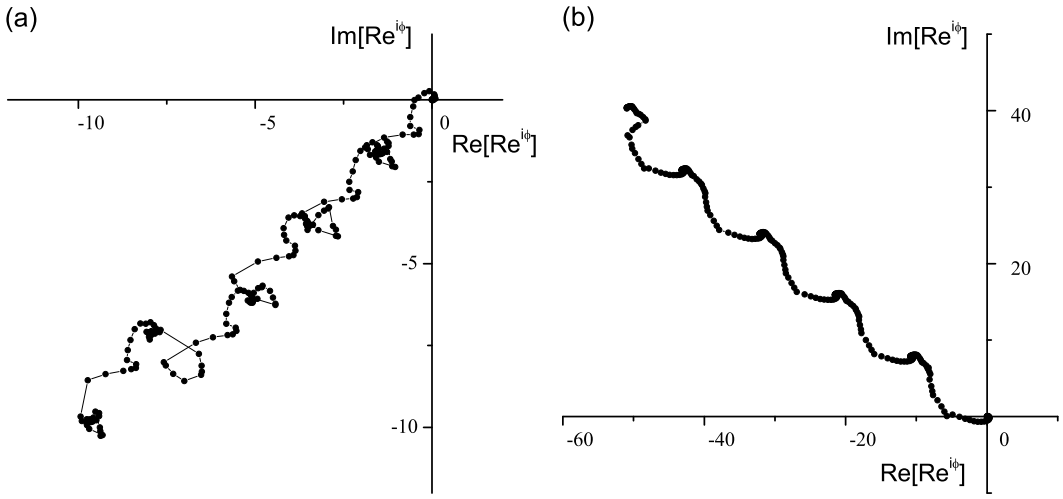

Fig. 5. (a)Vector chain for $x = -1.6$. (b)Vector chain for $x = 3.1$

packet, we can take a quite narrow initial wave function, such as $\psi(x_0, 0) = \delta(x_0 - x_i)$, sits at $x_i = 50$, of course it will rebuild itself at time $t = T_{rev}$. Then from equation (5) we see the wave function directly connect to the semiclassical propagator,

$$\begin{aligned}\psi(x,t) &= \int dx_0 G(x, x_0; t)\, \psi(x_0, t) \\ &= \int dx_0 G(x, x_0; t)\, \delta(x_0 - x_i) = G(x, x_0; t)\,. \end{aligned} \tag{14}$$

Referring to the existing works on Feynman path integral in infinite square well [24,25], the semiclassical propagator can be written as a summation of contributions from all the stationary phase points

$$\begin{aligned}G(x, x_0; t) =& \sqrt{\frac{m}{2\pi i\hbar t}} \left[\sum_{n=-\infty}^{\infty} \exp\left(\frac{im\left(-x - x_0 + 2nL\right)^2}{2\hbar t} - i\left|2n-1\right|\pi \right) \right. \\ &\left. + \sum_{n=-\infty}^{\infty} \exp\left(\frac{im\left(x - x_0 + 2nL\right)^2}{2\hbar t} - i\left|2n\right|\pi \right) \right] \\ =& \sqrt{\frac{m}{2\pi i\hbar t}} \left[\sum_{n=-\infty}^{\infty} \exp\left(\frac{im\left(x - x_0 + 2nL\right)^2}{2\hbar t} \right) \right. \\ &\left. - \sum_{n=-\infty}^{\infty} \exp\left(\frac{im\left(-x - x_0 + 2nL\right)^2}{2\hbar t} \right) \right] \end{aligned} \tag{15}$$

Fig 1 (b) shows part of the manifold at time T_{rev} which evolves from initial δ wave function, the intersection of $x = x_t$ with manifold produces stationary phase points. The two sums in Eq. 15 correspond to stationary phase points with classical trajectories bouncing off the wall by even and odd times respectively. To simplify the Eq. 15, we use the Jacobi theta function $\vartheta_3(z, T) =$

$\sum_{n=-\infty}^{\infty} \exp\left[i\left(\pi n^2 T + 2nz\right)\right]$ and its important property [26]

$$\vartheta_3\left(z,T\right) = \sqrt{i/T}\exp\left(z^2/i\pi T\right)\vartheta_3\left(z/T,-1/T\right), \tag{16}$$

the semiclassical propagator becomes

$$\begin{aligned} G\left(x,x_0;t\right) =& \frac{1}{2L}\left[\vartheta_3\left(\frac{\pi\left(x-x_0\right)}{2L},\frac{-\pi\hbar t}{2mL^2}\right) - \vartheta_3\left(\frac{-\pi\left(x+x_0\right)}{2L},\frac{-\pi\hbar t}{2mL^2}\right)\right] \\ =& \frac{1}{2L}\sum_{n=-\infty}^{\infty}\exp\left(\frac{-in^2\pi^2\hbar t}{2mL^2}\right)\left[\exp\left(\frac{in\pi\left(x-x_0\right)}{L}\right)\right. \\ & \left.-\exp\left(\frac{-in\pi\left(x+x_0\right)}{L}\right)\right] \\ =& \frac{2}{L}\sum_{n=1}^{\infty}\exp\left(\frac{-in^2\pi^2\hbar t}{2mL^2}\right)\sin\left(\frac{n\pi x_0}{L}\right)\sin\left(\frac{n\pi x}{L}\right). \end{aligned} \tag{17}$$

This is identical to the usual quantum propagator in infinite square well. At the revival time $T_{rev} = 4mL^2/\hbar\pi$ the wave function can be rewritten as

$$\begin{aligned} \psi\left(x,T_{rev}\right) =& G\left(x,x_0;T_{rev}\right) \\ =& \frac{1}{2L}\sum_{n=-\infty}^{\infty} e^{-i2n^2\pi}\left[\exp\left(\frac{in\pi\left(x-x_0\right)}{L}\right)\right. \\ & \left.+\exp\left(\frac{-in\pi\left(x+x_0\right)}{L}+i\pi\right)\right] \\ =& \frac{1}{2L}\sum_j e^{i\phi_j}. \end{aligned} \tag{18}$$

We can compare analytically the difference between low and high amplitude points of wave function. Taking $x_1 = 20, x_2 = 50$ for example, we find that for the high amplitude position at $x = 50$, the exponential functions $\exp\left(i\phi_j\right)$ in the summation distribute uniformly in complex plane. There are only eight phase terms [see Fig 2 (a)] in the sum. We need to distinguish the phase terms come from different exponential function in Eq. 18. The second exponential function gives out all 8 different terms distribute symmetrically around the circle so that they will cancel each other, whereas, the first exponential function only gives out $\phi = 0$ terms, they will build up big contributions and give out high amplitude. For the low amplitude point $x = 20$, however, both exponential functions generate 16 symmetrically distributed terms [see Fig 2 (b)] on the unit circle and therefore the summation approaches zero. Hence the interference between part of different classical trajectories yields the revival of wave packet.

Now we come to see a more general system, the Morse potential. It is also a widely used model in many fields. We take $V\left(x\right) = D\left[1-\exp\left(-\lambda x\right)\right]^2$

with $D = 150, \lambda = 0.288$, its revival time $T_{rev} = 2m\pi/(\hbar\lambda)^2$ can be derived by expanding the wave function with eigen functions of Morse potential, too [see Appendix A]. With 300 cells in x and 600 cells in p been used in the calculation, the semiclassical wave functions originate from $\psi(x_0, 0) = \sqrt{\gamma/\pi}\exp\left[-\gamma(x_0 - x_i)^2\right]$ $(\gamma = 2, x_i = 3.5)$ are pictured in Fig 3. Comparing to the FFT exact wave functions we can see semiclassical wave functions agree well for different time scales. In Fig 3 we plot the normalized classical coordinate space density arising from the initial classical distribution. Since the semiclassical result consists of the square root of classical probabilities multiplied by phase terms and added together, but it is easy to construct its purely classical result by removing the phase terms, and squaring and adding all the square root classical densities.

It is surprising that despite the fact that the classical trajectories are spread all over the available phase space and coordinate space, the semiclassical approximation can still build a localized wave packet at the revival time T_{rev}.

In order to demonstrate the relationship between semiclassical wave function and classical information carried by trajectories, we first Wigner transform the initial Gaussian distribution $\psi(x) = \sqrt{\gamma/\pi}\exp\left[-\gamma(x - x_i)^2\right]$,

$$\begin{aligned} W(x,p) =& \frac{1}{\pi\hbar}\int_{-\infty}^{\infty}\psi^*(x-s)\,\psi(x+s)\,e^{i2ps/\hbar}ds \\ =& \frac{\gamma}{\pi^2\hbar}\int_{-\infty}^{\infty}e^{-\gamma(x-x_i-s)^2}e^{-\gamma(x-x_i+s)^2}e^{i2ps/\hbar}ds \\ =& \frac{\gamma}{\pi^2\hbar}\int_{-\infty}^{\infty}e^{-2\gamma(x-x_i)^2-2\gamma s^2+i2ps/\hbar}ds \\ =& \sqrt{\frac{\gamma}{2\pi^3\hbar^2}}e^{-p^2/2\gamma\hbar-2\gamma(x-x_i)^2}, \end{aligned} \tag{19}$$

which remains a Gaussian. Then we plot the evolution of this Wigner distribution in phase space after revival time T_{rev} in Fig 4. The starting swarm of classical trajectories emerges as an elliptical disk; as time evolves this ellipse stretches and twists, forming a large whorl. (Indeed, the time evolution of the phase space is that of an area preserving twist map).

It might appear that the vertical sections of the classical manifolds on the left and right sides of the whorl would dominate the contribution to the semiclassical wave function for two reasons: First, the prefactor $1/\sqrt{|\partial x/\partial p_0|}$ in VVG propagator in equation (2) is large for this part of the manifold. This is because the density of the distribution is proportional to the probability $1/\sqrt{|\partial x/\partial p_0|}$ of classical particles locating at those regimes. Second, these particles have similar classical actions [see Fig 4 (a)]. In Appendix B we prove the classical action difference between two points equals the enclosed area of

the manifold. Near the fold regimes small enclosure areas lead to similar classical actions. The abrupt changes of color at the turning points indicate the change of Maslov index at those points. The combination of these two factors yields large result refers to equation (2). In Fig 4 (b) we blurred the phase space diagram for an intuitive view. The whorl average out and give neutral gray colors everywhere except where the revival is occurring. When combined along vertical lines, those regions with monochromatic bright colors will give out the revival wave packet.

Nevertheless, one could still doubt why we don't get a high amplitude wave function at positions of folds on left side, they also meet the conditions list above. To compare the difference, we write the formula of the wave function into a compact form:

$$\begin{aligned}\psi(x,t) &= \int dx_0 G(x,x_0;t)\,\psi(x_0,0) \\ &= \left(\frac{1}{2\pi i\hbar}\right)^{1/2} \int dx_0 \sum_j \left|\frac{\partial x}{\partial p_0}\right|^{-1/2} \exp\left[\frac{iS_j(x,x_i)}{\hbar} - i\upsilon_j\pi\right]\psi(x_0,0) \\ &= \int dx_0 R e^{i\phi} = \sum_n R_n e^{i\phi_n}\Delta x_0.\end{aligned} \tag{20}$$

We can approximate the quadrature numerically by a finite sum of complex vector. We divide x space into hundreds of sections, and evaluate the vector separately in each section. By drawing each vector from the tips of previous vector, the summation will form a chain, and the line drawn from first point to the end point represent the quadrature. We draw two chains respectively for $x = -1.6$ and $x = 3.1$ in Fig 5.

For the low amplitude region $x = -1.6$, in the vicinity of destructive interference, the chain circles continuously, and results in a small total vector [see Fig 5 (a)]. This indicates the phase of stationary phase points changes only slightly and continuously, leading to destructive interference between classical trajectories and a small amplitude of wave function. A different situation applies in Fig 5 (b) for the position $x = 3.1$. Here the small phase difference between stationary points accumulates a persistent growth of the total vector, viz. the constructive interference produces high amplitude of wave function.

4 Conclusions and discussion

Whenever and wherever they apply, semiclassical methods can be extremely useful not only in computations, but in providing an underlying intuition for quantum phenomena. Here we have shown that something so subtle as

a quantum revival still has classical underpinnings, as seen by the successful construction of the phenomenon using only classical mechanics as input. Semiclassical methods are accurate enough to describe the quantum revival phenomenon. The quantum revival phenomenon does not stem from an accumulation of classical trajectories. Rather, the classical trajectories are rather uniformly spread, and it is through destructive interference of the semiclassical amplitudes that the wave function is canceled in most places.

Of course, this is a momentary phenomenon, in the sense that beyond the revival time the way packet will again begin to spread and become quite delocalized quantum mechanically. However, imagine the following scenario: at the moment of a revival, with the wave packet built up on one side of the potential, suppose a time-dependent barrier is erected, preventing the wave packet from any immediate penetration beyond the barrier. If the barrier remained up, and the potential were sufficiently asymmetric and designed properly the quantum mechanical wave packet would remain on one side of the barrier forever. This raises an even more interesting and challenging question: When the time-dependent barrier was raised, this traps classical manifolds on the "empty" side of the barrier. Presumably at the moment of the trapping, the semiclassical wave function would indeed be correctly exceedingly small at that point, but for how long could this semiclassical result correctly describe the fact that the wave function never reappeared in that region? One could call this the "semiclassical propagation of nothing". That is to say, abstracting this a little further, suppose you begin with a quite complex set of classical manifolds, interpreted semiclassically, which gives essentially zero semiclassical wave function everywhere. Now, the continued semiclassical propagation of these manifolds should continue to give a vanishingly small function. Any errors in the semiclassical propagation will cause wave function amplitude to appear incorrectly.

While we cannot fully explain the situation here, we believe this phenomenon may be affecting the quantum classical correspondence in branched electron flow [27]. Branched electron flows are usually ascribed to a purely classical effect [27,28]; however, classical and quantum electron flows begin to disagree, with some branches suddenly missing in the quantum result as compared to the classical, as one moves further and further from the source of electrons. In the future we hope to verify our conjecture that the missing branches are an effect of destructive interference of classical trajectories, by using semiclassical methods.

5 Acknowledgements

One of us (Z. X. Wang) would like to acknowledge helpful discussions with Brian Landry. This work was supported in part by the National Natural Science Foundation of China (Grant Nos.10574121 and 10874160), '111' Project, Chinese Education Ministry and Chinese Academy of Sciences.

A Appendix A

For Morse potential $V(x) = D\left[1-\exp(-\lambda x)\right]^2$, one can express the time dependent wave function in terms of eigen functions $\varphi_n(x)$, via

$$\psi(x,t) = \sum_{n=0}^{\infty} a_n \varphi_n(x) e^{-iE_n t/\hbar}, \tag{A.1}$$

where the eigen values are $E_n = \alpha(n+1/2) - \beta(n+1/2)^2$ with $\alpha = \hbar\lambda\sqrt{2D/m}$, $\beta = \hbar^2\lambda^2/2m$. The revival condition $\psi(x,T) = \psi(x,0)$ requires

$$E_n T = \left[\alpha(n+1/2) - \beta(n+1/2)^2\right] T = 2M_n\pi, \tag{A.2}$$

where M_n are integers. Make a subtraction of adjacent n of equation (A.2) gives

$$(\alpha - 2\beta n - 2\beta) T = 2K_n\pi, \tag{A.3}$$

with K_n are also integers. Then apply the subtraction of adjacent of equation (A.3) again, we get the equation for the shortest revival time T_{rev} is

$$2\beta T_{rev} = 2\pi. \tag{A.4}$$

So we have the revival time $T_{rev} = \pi/\beta = 2m\pi/(\hbar\lambda)^2$.

B Appendix B

We ought to prove the difference of classical action S_A and S_B equals to the shade area Q_1. First we look at point B and C. From classical action formula $S = \int p(q)\,dq + \int H(p,q)\,dt$ we have $\partial S/\partial q = p$, thus the action difference from B to C is

$$S_C - S_B = \int_B^C \frac{\partial S}{\partial q} dq = \int_B^C p dq = area Q_2. \tag{B.1}$$

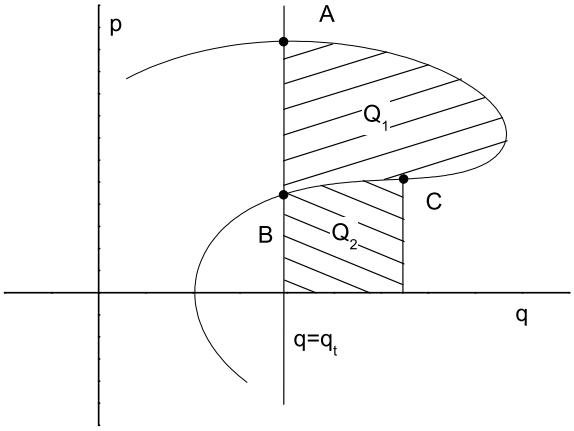

Fig. B.1. Classical manifold. The area contained between intersections of the manifold $p(q)$ and a position state (vertical line $q = q_t$) is Q_1.

Then, in a similar way

$$S_A - S_B = \int_B^A \frac{\partial S}{\partial q} dq = \int_B^A p dq = area Q_1. \tag{B.2}$$

References

[1] J. H. Eberly, N. B. Narozhny, J. J. Sanchez-Mondragon, Phys. Rev. Lett. 44 (1980) 1323.

[2] N. B. Narozhny, J. J. Sanchez-Mondragon, J. H. Eberly, Phys. Rev. A 23 (1981) 236.

[3] J. Parker, C. R. Stroud, Jr., Phys. Rev. Lett. 56 (1986) 716.

[4] J. Parker, C. R. Stroud, Jr., Phys. Scr. T12 (1986) 70.

[5] G. Alber, P. Zoller, Phys. Rep. 199 (1991) 231.

[6] I. Fischer, D.M. Villeneuve, M. J. J. Vrakking, A. Stolow, J. Chem. Phys. 102 (1995) 5566.

[7] M. J. J. Vrakking, D. M. Villeneuve, A. Stolow, Phys. Rev. A 54, (1996) R37.

[8] M. A. Doncheski, R. W. Robinett, Ann. Phys. 308 (2003) 578.

[9] D. L. Aronstein, C. R. Stroud, Jr., Phys. Rev. A 62, (2000) 022102.

[10] S. I. Vetchinkin, V. V. Eryomin, Chem. Phys. Lett. 222 (1994) 394.

[11] R. W. Robinett, Am. J. Phys. 68 (2000) 410.

[12] D. F. Styer, Am. J. Phys. 69 (2001) 56.

[13] S. Waldenstrom, K. Razi Naqvi, K. J. Mork, Phys. Scr. 68 (2003) 45.

[14] R. W. Robinett, Phys. Rep. 392 (2004) 1.

[15] S. Tomsovic,E. J. Heller, Phys. Rev. Lett. 67 (1991) 664.

[16] S. Tomsovic,E. J. Heller, Phys. Rev. E 47 (1993) 282.

[17] L. Kaplan, E. J. Heller, Phys. Rev. Lett. 76 (1996) 1453.

[18] E. J. Heller, J. Chem. Phys. 62 (1975) 1544.

[19] R. G. Littlejhon, Phys. Rep. 138 (1986) 193.

[20] E. J. Heller, J. Chem. Phys. 94 (1991) 2723.

[21] M. C. Gutzwiller, J. Math. Phys. 8 (1967) 1979.

[22] W. H. Miller, J. Phys. Chem. A 105, 2942 (2001).

[23] M. D. Feit, J. A. Fleck Jr., A. Steiger, J. Comp. Phys. 47 (1982) 412.

[24] M. Goodman, Am. J. Phys. 49 (1981) 843.

[25] C. Grosche, F. Steiner, Handbook of Feynman path integrals (Springer, New York, 1998)

[26] M. Abramowitz, I. A. Stegun, Handbook of mathematical functions with formulas, graphs, and mathematical tables (U. S. Government Print Office, Washington, 1964)

[27] M. A. Topinka, B. J. LeRoy, R. M. Westervelt, S. E. J. Shaw, R. Fleischmann, E. J. Heller, K. D. Maranowski, A. C. Gossard, Nature 410 (2001) 183.

[28] E. J. Heller, Scot Shaw, Inter. J. Mod. Phys. B 17 (2003) 3977.